Electron Spin Resonance using DPPH
&
Study of Magnetic Resonance with Compass

Aryan Shrivastava*
School of Physical Sciences, National Institute of Science Education and Research
(Dated: October 3, 2025)

This study investigates magnetic resonance through two complementary experiments: electron spin resonance (ESR) in a DPPH crystal and classical resonance in a compass. We observed resonant energy absorption in DPPH at radio frequencies and determined the Landé g-factor, g $= 1.925 \pm 0.008$, showing a 3.9% deviation from the literature value. In the compass experiment, we demonstrated resonant excitation by matching the drive frequency to the needle's natural precession frequency. Both experiments successfully illustrate the universal nature of magnetic resonance across quantum and classical systems.

I. OBJECTIVE

1. Study the resonance peaks of DPPH
2. Calculate the Landé g-factor
3. Study magnetic resonance through a compass

II. THEORY

A. Elementary Magnetic Resonance

When a magnetic moment μ is placed in a static magnetic field H_0, it precesses about the field with the *Larmor frequency*[1]

$$\omega_0 = \frac{egH_0}{2mc}, \tag{1}$$

where e is the electron charge, m is its mass, c is the speed of light, and g is the Landé g-factor. This precessional motion is shown in Fig. 1(a).

If an additional weak oscillating magnetic field H_1 is applied in the plane perpendicular to H_0 with angular frequency ω_1, resonance occurs when

$$\omega_1 = \omega_0. \tag{2}$$

In this condition, the system absorbs energy efficiently, and the magnetic moment undergoes nutation (Fig. 1(b)).

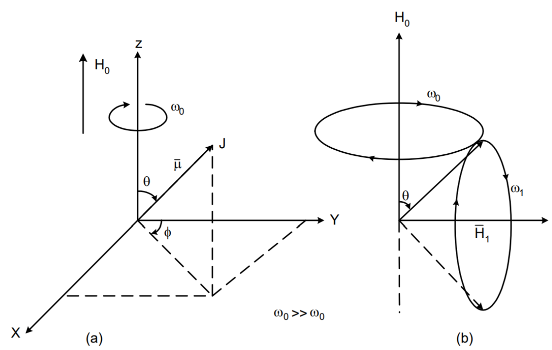

FIG. 1. Precession of a magnetic moment μ when placed in a magnetic field H_0
(a). The spin precesses with angular frequency $\omega_0 = \gamma H_0$; the angle θ is a constant of the motion.
(b). In addition to H_0 a weak magnetic field H_1 is now also applied. H_1 is rotating about the z axis with angular frequency ω_0 and therefore μ precesses about H_1 with angular frequency $\omega_1 = \gamma H_1$; θ is not any more conserved.

B. Quantum Description of ESR

In the quantum picture, an electron with spin S and orbital angular momentum L couples to form a total angular momentum J. In a magnetic field H_0, the $2J + 1$ sublevels are separated in energy by

$$\Delta E = g\mu_B H_0, \tag{3}$$

where μ_B is the Bohr magneton.

Resonance occurs when the applied radio-frequency (RF) field of frequency ν_1 satisfies

$$\Delta E = g\mu_B H_0 = h\nu_1 = h\nu_0 \tag{4}$$

This is equivalent to the classical resonance condition $\omega_1 = \omega_0$. The allowed transitions obey the magnetic dipole selection rule

$$\Delta m = \pm 1. \tag{5}$$

The fine structure splitting and allowed transitions are illustrated in Fig. 2.

C. ESR in Solids

In paramagnetic solids, electron spins interact with one another and with the lattice:

* aryan.shrivastava@niser.ac.in

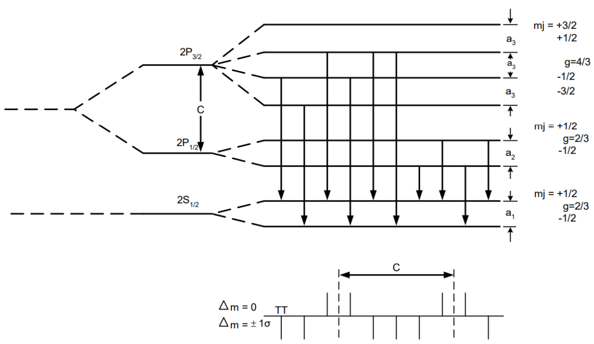

FIG. 2. Energy levels of a single valence electron atom showing a P state and an S state under the influence of an external magnetic field. The structure of the line shown in lower part of the figure.

- **Spin–Spin interaction:** the spin interacts with a neighbouring spin, but the total energy of the spin system remains constant.
- **Spin–Lattice interaction:** spins exchange energy with the lattice, which serves as a thermal reservoir.

According to the Boltzmann distribution, lower-energy spin states are more populated. Thus, when resonance is achieved, absorption occurs as the RF field drives transitions between these states.

D. Relaxation and Saturation

Relaxation is the process through which spins return to equilibrium after excitation. Two characteristic times are defined:

- Spin–spin relaxation time, T_2: redistribution of energy within the spin system.
- Spin–lattice relaxation time, T_1: transfer of energy from spins to the lattice.

If the RF power exceeds the relaxation capability, absorption saturates and further net energy absorption ceases.

E. Line Width

The ESR absorption line width arises due to interactions that broaden the energy levels. It is inversely related to relaxation times:

$$\Delta H \sim \frac{1}{T_2} + \frac{1}{T_1}. \tag{6}$$

Spin–spin interactions are usually dominant and determine the observed line width.

F. Resonance Condition and g-factor

The fundamental ESR condition is

$$h\nu_1 = g\mu_B H_0. \tag{7}$$

From this, the Landé g-factor can be calculated as

$$g = \frac{h\nu_1}{\mu_B H_0}, \tag{8}$$

where h is Planck's constant and μ_B the Bohr magneton.

G. ESR with DPPH Sample

In this experiment, the standard sample is **DPPH** (2,2-diphenyl-1-picrylhydrazyl), a stable free radical widely used for ESR calibration.. The ESR spectrum is observed using a radio-frequency oscillator and Helmholtz coils.

The magnetic field at the center of the Helmholtz coils is

$$H = \left(\frac{4}{5}\right)^{3/2} \frac{\mu_0 n I}{a}, \tag{9}$$

where n is the number of turns in each coil, a the radius of the coil, and I the current.

The resonance peaks (four in total due to modulation and symmetry, Fig. 3) correspond to absorption dips.

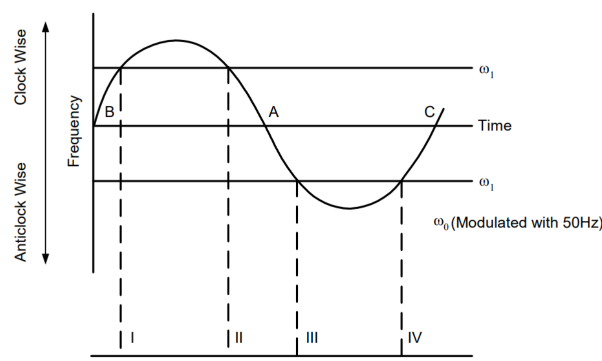

FIG. 3. The applied radio frequency field is linearly polarised and can be represented as two oppositely rotating circularly polarised fields. Since the static magnetic field H_0 also changes direction, resonance occurs when $\omega_1 = \omega_0$ in both magnitude and direction, giving four resonances in each full cycle of H_0.

H. Magnetic Resonance using Compass

Magnetic resonance [2] describes the resonant interaction of spins with electromagnetic fields. In this tabletop experiment, a compass needle (treated as a magnetic dipole of moment $\vec{m}$) is subject to the field of a permanent magnet $\vec{B}_{PM}$ and a weak alternating drive field $\vec{B}_{\text{drive}}$ from a coil. The torque on the needle is

$$\vec{\tau} = \vec{m} \times \left(\vec{B}_{PM} + \vec{B}_{\oplus} + \vec{B}_{\text{drive}} \right). \tag{10}$$

Since the permanent magnet dominates, the Earth's field $\vec{B}_{\oplus}$ is neglected. The dynamics reduce to

$$\vec{m} \times \left(\vec{B}_{PM} + \vec{B}_{\text{drive}} \right) = J\ddot{\theta}\,\hat{z}, \tag{11}$$

where J is the moment of inertia of the needle and θ its angular deflection.

Expanding in small-angle approximation yields the driven harmonic oscillator equation

$$\ddot{\theta} + \omega_0^2 \theta = \omega^2, \tag{12}$$

with natural and drive frequencies

$$\omega_0 = \sqrt{\frac{mB_{PM}}{J}}, \qquad \omega = \sqrt{\frac{mB_{\text{drive}}}{J}}. \tag{13}$$

Resonance occurs when $\omega = \omega_0$, leading to maximum oscillation amplitude of the needle.

The magnetic field of the permanent magnet in the dipole approximation depends on distance d as

$$B_{PM} = \frac{\mu_0}{4\pi} \frac{2m_{PM}}{d^3}, \tag{14}$$

where m_{PM} is the dipole moment of the permanent magnet. Substituting into the resonance condition gives the resonant frequency

$$f_{\text{res}} = \frac{1}{2\pi} \sqrt{\frac{\mu_0}{2\pi} \frac{m_{PM}}{d^3} \frac{m}{J}}. \tag{15}$$

Thus, by varying the magnet–compass distance d, one tunes B_{PM} and observes resonance when the drive frequency matches the natural precession frequency of the compass needle.

III. EXPERIMENTAL APPARATUS

A. Electron Spin Resonance (ESR)

The ESR spectrometer consists of an RF oscillator with the DPPH sample in the induction coil, a pair of Helmholtz coils for field modulation, detection and amplification circuits, and an oscilloscope in XY mode. A gaussmeter is used to measure the magnetic field, and resonance peaks are observed as absorption dips.

B. Magnetic Resonance with a Compass

This setup uses a compass at the center of a circular coil, a permanent magnet providing a static field, and a function generator driving the coil with a low-frequency AC field. Resonance is detected as amplified oscillations of the compass needle when the drive frequency matches its natural precession frequency.

IV. OBSERVATIONS

In the ESR experiment with DPPH, the oscilloscope displayed characteristic absorption dips, whose positions shifted with changes in the coil current and frequency. The separation of peaks was used to determine the resonance field and calculate the Landé g-factor.

In the magnetic resonance with compass setup, the needle oscillations were monitored as the distance of the permanent magnet was varied. Small oscillations were observed for very weak or strong static fields, while pronounced resonance occurred at intermediate distances where the drive frequency matched the natural precession frequency.

TABLE I. ESR observations with DPPH sample at various frequencies (P = 14.6V).

I (mA)	Q (V)	H_{rms} (mT)	H_{pp} (G)	H_0 (G)	g	f (MHz)
99	4.28	0.50	16.35	4.79	1.851	12.41
127	3.20	0.66	20.97	4.59	1.932	
152	2.58	0.79	25.10	4.43	2.002	
181	2.16	0.95	29.89	4.42	2.006	
208	1.96	1.08	34.35	4.61	1.924	
234	1.76	1.21	38.64	4.65	1.907	
260	1.57	1.35	42.94	4.62	1.919	
286	1.43	1.48	47.23	4.63	1.916	
311	1.32	1.63	51.36	4.64	1.911	
99	4.72	0.50	16.35	5.29	1.851	13.70
126	3.70	0.66	20.80	5.27	1.857	
153	2.90	0.79	25.26	5.02	1.950	
181	2.42	0.95	29.89	4.95	1.978	
208	2.14	1.08	34.35	5.03	1.946	
233	1.90	1.21	38.48	5.01	1.954	
259	1.74	1.35	42.77	5.09	1.924	
285	1.60	1.48	47.06	5.16	1.897	
309	1.47	1.63	51.03	5.14	1.905	
99	5.15	0.50	16.35	5.77	1.908	15.41
127	4.12	0.66	20.97	5.92	1.860	
154	3.32	0.79	25.43	5.78	1.905	
181	2.74	0.95	29.89	5.61	1.963	
208	2.38	1.08	34.35	5.60	1.966	
235	2.10	1.21	38.81	5.58	1.974	
260	1.92	1.35	42.94	5.65	1.949	
285	1.78	1.48	47.06	5.74	1.918	
310	1.64	1.63	51.19	5.75	1.915	

TABLE II. Resonance observations for the compass experiment.

S. No.	f (Hz)	Distance (cm)	B (mT)
1	1.205	15.9	0.04
2	1.223	14.9	0.05
3	1.378	11.9	0.07
4	1.689	8.9	0.11
5	2.028	6.9	0.14
6	2.268	5.9	0.17
7	2.628	4.6	0.22
8	2.940	3.7	0.23

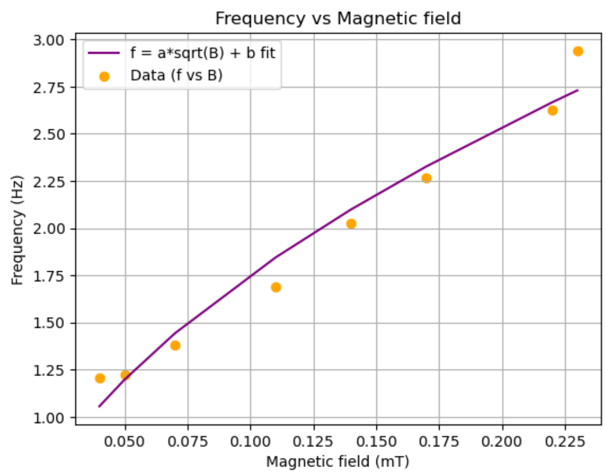

FIG. 4. Measured resonant frequency versus magnetic field for the compass experiment. The solid line shows a fit to $f = a\sqrt{B} + b$.

V. DATA ANALYSIS

A. Magnetic Resonance

The measured resonance frequency is plotted as a function of the applied magnetic field, as shown in Figure 4. The data exhibits a non-linear relationship, which is in qualitative agreement with the theoretical model of a driven harmonic oscillator for the compass needle. According to Eq. 15, the resonance frequency f_{res} is expected to be proportional to the square root of the static magnetic field strength, $f_{\text{res}} \propto \sqrt{B}$. The observed trend, where the frequency increases with the magnetic field in a non-linear manner, is consistent with this theoretical prediction.

However, the fit of the function $f = a\sqrt{B} + b$ to the data was poor, indicating a significant deviation from the ideal square-root dependence (see full code [3]. Potential sources of this error include the breakdown of the point-dipole approximation for the permanent magnet's field at close distances, friction in the compass needle's pivot, misalignment of the magnet and coil fields, and the difficulty in precisely determining the maximum oscillation amplitude at resonance by eye etc.

B. Calculating the Landé g-factor

The Landé g-factor for each measurement is obtained from the resonance condition

$$h\nu = g\,\mu_B H_0 \qquad \Longrightarrow \qquad g \;=\; \frac{h\nu}{\mu_B H_0}, \tag{16}$$

where h is Planck's constant, μ_B the Bohr magneton, ν the applied (resonance) frequency and H_0 the measured resonance field.

From the set of individual calculated values g g_i ($i = 1 \dots N$) we obtain the mean and the standard deviation of the sample. The arithmetic mean is

$$\overline{g} \;=\; \frac{1}{N}\sum_{i=1}^{N} g_i, \tag{17}$$

and the sample standard deviation is

$$\sigma_g \;=\; \sqrt{\frac{1}{N-1}\sum_{i=1}^{N}\big(g_i-\overline{g}\big)^2}. \tag{18}$$

$$\overline{g} = 1.92525 \;\approx 1.925, \tag{19}$$

$$\sigma_g = 0.04428 \;\approx 0.044. \tag{20}$$

C. Error Analysis

The uncertainty in the Landé g-factor can be estimated by using the standard deviation of the sample of calculated values. Instead of using the least count, we use the statistical spread of the observed values. The equation 18 provides the standard deviation of the 24 measurements. The uncertainty is given by the *standard error of the mean* (SEM) [4], defined as

$$\sigma_{\Delta g_{\text{avg}}} = \frac{\sigma_g}{\sqrt{N}} \approx 0.008$$

The percentage deviation of the experimental result from the literature value ($g_{\text{lit}} = 2.0036$) is calculated as:

$$\%\ \text{Deviation} = \left|\frac{1.925 - 2.0036}{2.0036}\right| \times 100\% = 3.92\%$$

The experimental value deviates from the literature value by approximately 3.9%, which is significantly larger than the experimental uncertainty of 0.4%. Also, the measured value is lower than the literature value, and the discrepancy lies outside the margin of experimental uncertainty. This indicates the presence of a systematic error, maybe in the calibration of the oscilloscope used to determine the resonance magnetic field H_0.

VI. RESULTS

The Landé g-factor for the DPPH free radical was determined experimentally from the electron spin resonance. The average value obtained from the measurements was:

$$\boxed{g_{\text{exp}} = 1.925 \pm 0.008}$$

This value can be compared to the accepted literature value for DPPH and a deviation of 3.9% was observed.

The Figure 4 confirmed the fundamental principle of magnetic resonance. The observed trend was qualitatively consistent with the expected non-linear relationship, $f_{\text{res}} \propto \sqrt{B}$, though quantitative deviations from the ideal model were observed.

VII. CONCLUSION

This experiment successfully demonstrated the fundamental principles of magnetic resonance through two distinct physical systems: the quantum spin system of DPPH and the classical magnetic dipole of a compass needle.

In the ESR investigation, the resonance condition was verified, resulting in an experimental Landé g factor of 1.925 ± 0.008 for the DPPH free radical. For the compass experiment, the resonant excitation of the needle was observed, with the measured resonance frequency showing the expected qualitative increase with the applied static magnetic field, confirming the driven harmonic oscillator model. The experiments effectively illustrated the universal nature of resonance as a phenomenon that bridges classical and quantum mechanical descriptions.

[1] National Institute of Science Education and Research. *ELECTRON SPIN RESONANCE USING DPPH*. NISER, 2024. Laboratory Manual for Modern Physics Experiments.

[2] National Institute of Science Education and Research. *Study of Magnetic Resonance with a Compass*. NISER, 2024. Laboratory Manual for Modern Physics Experiments.

[3] Aryan Shrivastava. P343—modern-physics-lab. `https://github.com/crimsonpane23/P343---Modern-Physics-lab.git`, 2025.

[4] John R. Taylor. *An Introduction to Error Analysis: The Study of Uncertainties in Physical Measurements*. University Science Books, Sausalito, CA, 2nd edition, 1997.